Behavior of Load-Bearing Reinforced Masonry Walls under Out-of-Plane Loading

Salem, Shady[1]; Ezzeldin, Mohamed[2]; El-Dakhakhni, Wael[3] and Tait, Michael[4]

ABSTRACT

The increases in accidental explosion events over the past two decades have demonstrated the urgent need to evaluate the behavior of blast-vulnerable structural components and develop subsequent risk mitigation strategies. In this context, several studies have focused on the out-of-plane behavior of either unreinforced masonry walls or non-load-bearing reinforced masonry shear walls (RMSW). However, to date, a limited number of studies have been conducted on the interaction between the axial load and out-of-plane demands (e.g. when subjected to blast loads) on such walls. As such, the current study focuses on investigating the out-of-plane behavior of seismically-detailed load-bearing RMSW with different designs. Experimental results of three scaled RMSW, with different axial stress levels, subjected to out-of-plane loading are presented. These results include the wall damage sequence, load-displacement response, stiffness degradation and energy dissipation. The current study extends the database of experimental results pertaining to load-bearing RMSW, to facilitate the development of relevant provisions within the next editions of relevant blast design standards.

KEYWORDS: *axial load, blast, experimental resistance functions, out-of-plane, reinforced masonry*

---

[1] Lecturer, Civil Engineering Department, The British University in Egypt, Cairo, Egypt, Shady.Salem@Bue.edu.eg
[2] Assistant Professor, Department of Civil Engineering, McMaster University, Hamilton, ON, L8S 4L7, Canada, ezzeldms@mcmaster.ca
[3] Professor, Department of Civil Engineering, McMaster University, Hamilton, ON, L8S 4L7, Canada, eldak@mcmaster.ca
[4] Professor, Department of Civil Engineering, McMaster University, Hamilton, ON, L8S 4L7, Canada, taitm@mcmaster.ca

INTRODUCTION

The advantages of reinforced masonry shear walls (RMSWs) have vouched for the application of such a system in numerous projects. The application of RMSWs is supported by their ease in construction and their in-plane ductile behavior when the walls are properly detailed according to the relevant design standards [1]. As such, the current North American codes (e.g. NBCC 2015, ASCE 2017) have included different seismic ductility categories [2,3]. However, RMSWs showed limited ductility and high vulnerability when loaded in the out-of-plane direction due to the mid-cell reinforcement configuration [4]. Moreover, the system robustness using different RMSWs in-plane ductility classifications showed high vulnerability for wall removal [5]. This out-of-plane loading can occur during multiple extreme events such as hurricanes, blasts, impact, etc. [6]. As such, this contradicting in-plane versus out-of-plane behavior of RMSWs may depict a trade-off in the application of the RMSWs system within the context of multi-hazard mitigation.

On the other side, the vast application of RMSWs in critical structures has necessitated the design of such structural components against blast. This demanding design is based on the increasing demand for blast-resistant structures especially after the 9/11 attacks [7]. As such, a comprehensive assessment of RMSWs subjected to an out-of-plane loading supported by an experimental result should be available to confirm a reliable design procedure. To date, available research has been limited only to non-load-bearing walls (i.e. no axial loads) with well-defined boundary conditions. For example, Bechara et al. (1996) tested six RMSWs under static out-of-plane four-point bending, however, ideal rollers were used and no axial loads were applied on these walls [8]. Moreover, Zhang et al. (2001) investigated the out-of-plane behavior of three flanged non-load-bearing RMSWs (i.e. supported on return walls at their ends); however, the configuration of such walls forced an atypical three-sided behavior [9]. Browning et al. (2011) reported the results of three non-load-bearing RMSWs supported on steel frames, which may not be a reasonable representation of current construction practice [10,11]. Similarly, Elsayed et al. (2016) tested three one-third scale non-load-bearing RMSWs under quasi-static loading, however, these walls were welded to a steel frame creating a special connection different than real masonry construction [12]. Finally, Porto et al. (2010) tested two systems of load-bearing perforated clay walls with adequate masonry to slab connection (i.e. similar to the real construction connections), however, the used masonry does not represent the concrete masonry units used in North American construction practices [13,14].

The current study experimentally investigates the out-of-plane behavior of three half-scaled RMSWs, originally designed and detailed for in-plane seismic load resistance. The walls are loaded with uniformly distributed out-of-plane loads as well as axial load. The experimental program including the construction and testing phases as well as the results are thoroughly elaborated. The results include the wall damage sequence, load-displacement response, stiffness degradation, and energy dissipation. The current study extends the database of experimental results pertaining to load-bearing RMSW, to facilitate the development of relevant provisions within the next editions of relevant blast design standards

EXPERIMENTAL PROGRAM

The test matrix included three typical walls with different axial loads. All walls were subjected to a displacement-controlled quasi-static out-of-plane cyclic loading until they reached a strength degradation to 70% of the maximum strength to capture the post-ultimate strength behavior. The load-bearing walls were designed to maintain their axial load levels throughout the test while loaded in the out-of-plane direction using uniformly distributed loads across the wall's surface area. The following subsections provide details on the wall selection, material properties, test setup, instrumentation and loading protocol.

Test Matrix
The experimental program focused on testing three half-scale walls with 1,420 mm length, 90 mm thickness, 2,000 mm height and 1500 mm loading span. The 500 mm difference between the total wall height (2000 mm) and the loaded wall span (1500 mm), is to realistically simulate the reinforcement development length within the upper building floors, as shown in Fig. 1(b). The walls were originally designed to represent the current in-plane seismic classifications (i.e. ordinary, intermediate and special) of RMSWs [3]. The main variable within the three tested RMSWs, is the axial load level. The axial stress levels vary from 0% to 15% of the axial compressive strength. The walls are identified in this study using numbers that represent the axial stress ratio (i.e. 0, 5,15%). For example, Wall 05 is loaded with an axial stress ratio of 5% of its cross-section area. The vertical reinforcement ratio (ρ_v) is 0.61% of the vertical gross area, while the horizontal reinforcement ratio(ρ_h) is 0.14%. It worth mentioning that the axial stress was limited to 15% of the walls axial capacity to simulate a real case scenario of a wall bearing system with an average slab spans equal to 6m. Fig. 1a shows the cross-sections and reinforcement details of the tested walls, while Table 1 summarizes their vertical and horizontal reinforcement ratios as well as their in-plane ductility classifications according to the TMS [3]. Table 1 also summarizes the out-of-plane wall section classification based on sectional analysis. In this analysis, a concrete model with a crushing stain of 0.0025 as per CSA S304 [2]and a monotonic stress-strain relationship for the vertical reinforcement were adopted and applied within Bernoulli's principle (i.e. linear strain distribution) were assumed [3,15].
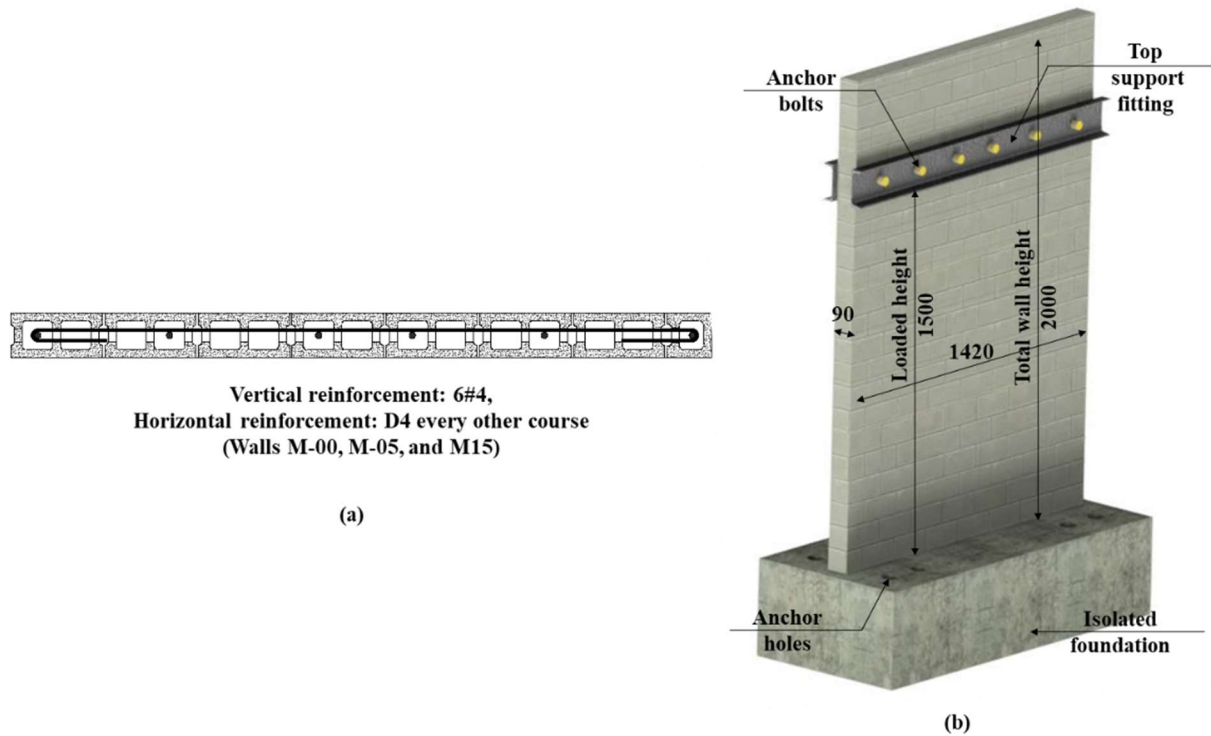
Wall Details and Construction
The walls were constructed using half-scale concrete masonry units (CMU) units in a running bond pattern and face shell mortar bedding by certified masons, following the North American construction practices. The (90x90x185 mm) half-scale CMU units were resembling the standard two-cell 190mm full-scale CMU [16]. The scaled CMU were saw cut to 25 mm deep through their webs to allow the placement of the horizontal reinforcement. Each wall was constructed on a 1500 mm x700 mm isolated reinforced concrete foundation with a thickness of 400 mm. The construction of the walls was conducted with a running bond scheme using approximately 5-mm-thick mortar joints representing the scaled version of the common 10 mm joints in full-scale masonry construction. The vertical reinforcements were extended to the full height of their

corresponding walls with no splices. The vertical reinforcements were also bent 90-degrees and tied to the lower mesh of the foundation with an extended leg of 150 mm, to ensure a full development length. The walls were constructed and grouted in two stages to facilitate the low-lift grouting technique [3]. The walls were grouted with fine grout having weight mixing portions of 1: 0.04: 3.9: 0.85 (Portland cement: lime: dry sand: water) with an average slump of 230mm. Horizontal D4 reinforcements were placed on top of the CMU notches with a 180-degree standard hook around the vertical edge rebars [17], as shown in Fig. 1a. It worth mentioning that the D4 reinforcement was heat-treated to enhance its ductility based on the available literature [18]. To simulate a typical continuous wall loaded in the first story, the wall was horizontally supported at 1,500 mm from its base, resembling a scaled version of a first story wall with 3,000 mm height. With regard to the top horizontal support, the walls were drilled and threaded bars were fitted/fixed using a non-shrinkable epoxy at the location of the support following the standard grouting and anchorage procedure of the American Concrete Institute [19]. Fig. 1b shows the typical three-dimensional view of the tested walls illustrating the tested area and the location of the top support. Moreover, the full sequence of construction is depicted in Figure 2.

Table 1. Details of the test matrix

| Wall | Vertical reinforcement | | Horizontal reinforcement | | MSJC (2013) classification | Out-of-plane classification |
	Number and size	ρ_v (%)	Number and size	ρ_h (%)		
M-00	6 No. 4 (6 x 129 mm^2)	0.61	D4 every other course (25mm^2 @ 200mm)	0.14	Special	Under-reinforced
M-05	6 No. 4 (6 x 129 mm^2)	0.61	D4 every other course (25mm^2 @ 200mm)	0.14	Intermediate	Under-reinforced
M-15	6 No. 4 (6 x 129 mm^2)	0.61	D4 every other course (25mm^2 @ 200mm)	0.14	Ordinary	Over-reinforced

Forty-three blocks for stretchers and seven blocks for half units were randomly selected and tested according to the ASTM C140-16 [20] and CSA A165 [21]. The average compressive strengths −based on net area− were 14.5 (c.o.v = 14.1%) and 16.4 MPa (c.o.v = 6.7%) for the stretchers and half units, respectively. Pre-blended, pre-packaged, type S-mortar was used with an average flow of 126%. The average compressive strength of the used mortar, based on thirty standard mortar cubes taken from each batch during the construction, was 19.2 MPa (c.o.v = 21.2 %) [22,23]. Twenty-three grout cylinders were tested and resulted in 21.3 MPa average strength(c.o.v = 15.1%) [23,24]. Sixty-nine fully grouted running bond masonry prisms were tested −one block long and four blocks height− to evaluate the grouted masonry compressive strength normal to the bed joint. The average compressive strength was 11.8 MPa (c.o.v = 13.4%); which results in 13.5 MPa standard average compressive strength −by multiplying the suggested correction factor of 1.15 – to account for the tested height-to-thickness ratio [25].

Figure 1: Tested walls: (a) Typical cross-sections; (b) 3D view for a typical wall (all dimensions are in mm)

The tensile test was conducted for the used rebars – # 4 (used as the vertical reinforcement), D4 (used as horizontal reinforcement), and M10 (used in the foundation) [26] in order to determine their yield and ultimate strengths. The average yield strength of the M10 rebars (100 mm^2) was 436 MPa (c.o.v = 1.32%), whereas the average yielding strength of the #4 (129 mm^2), and the D4 (45 mm^2) rebars were 459, 436 and 517 MPa (c.o.v = 4.6,0.92 and 6.9%) respectively. It should also be mentioned that the D4 reinforcement was heat-treated to lower its yielding strength and increase its ductility based on the available literature [18].

Test setup, Instrumentation and Loading Protocol
The test setup was designed to simulate the application of uniformly distributed out-of-plane loads on the load-bearing walls simultaneously with a uniform (and constant) axial load (P_A). The out-of-plane distributed loads were applied through a displacement-controlled (main) actuator with 500 kN capacity and 500 mm stroke. This actuator was exerted to the walls through nine-point/patch loads (300 mm x 300 mm) using nine (secondary) actuators, as shown in Fig. 2a. These actuators were connected in a closed-loop hydraulic system to equate the applied forces and allow for different displacements without restrictions on the RMSWs deformations. The position of the swivel end of the main actuator was fixed in order to maintain the location of the resultant force at the center of mass of the wall-loaded area, while the nine secondary actuators were pinned to a rigid steel frame supported on the main actuator. The nine actuators were capped with steel ball-

bearing ends to allow for the rotation of the loading pads on the tested walls. The loading pads consist of 200 mm x 200 mm rigid steel plates of 250 mm thickness and buttressed with 300 mm x 300 mm rubber pads of 40 mm thickness, in order not to restrain the wall deformations.
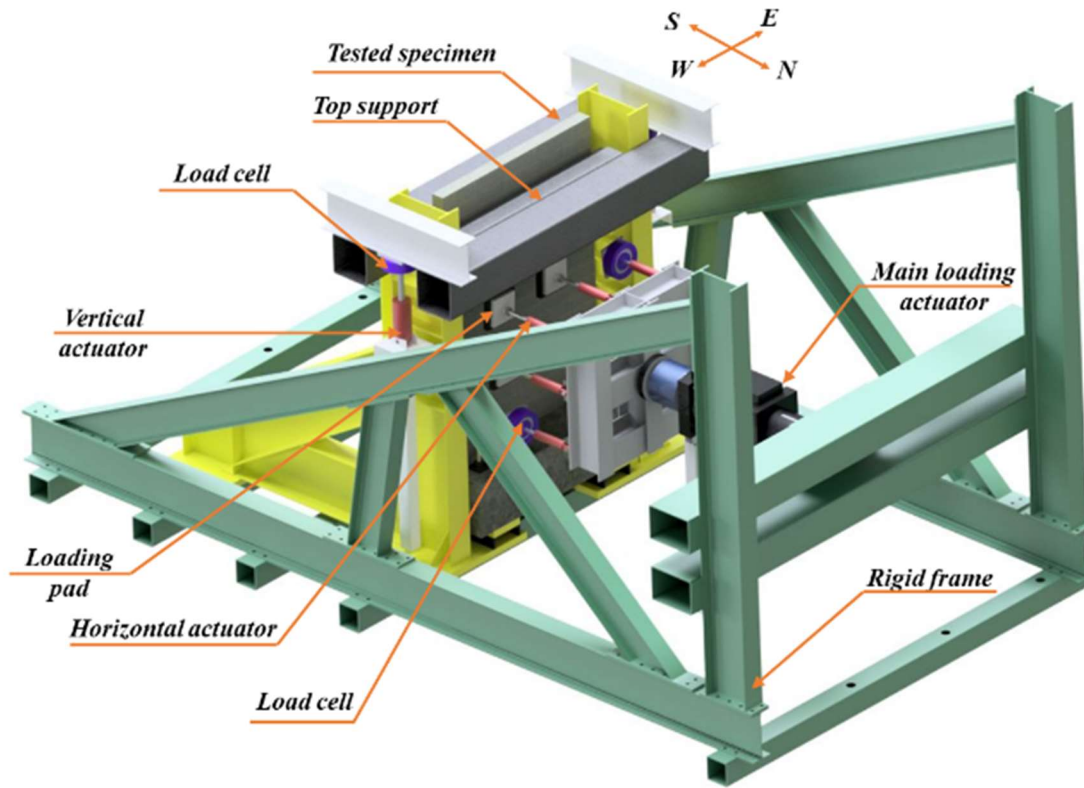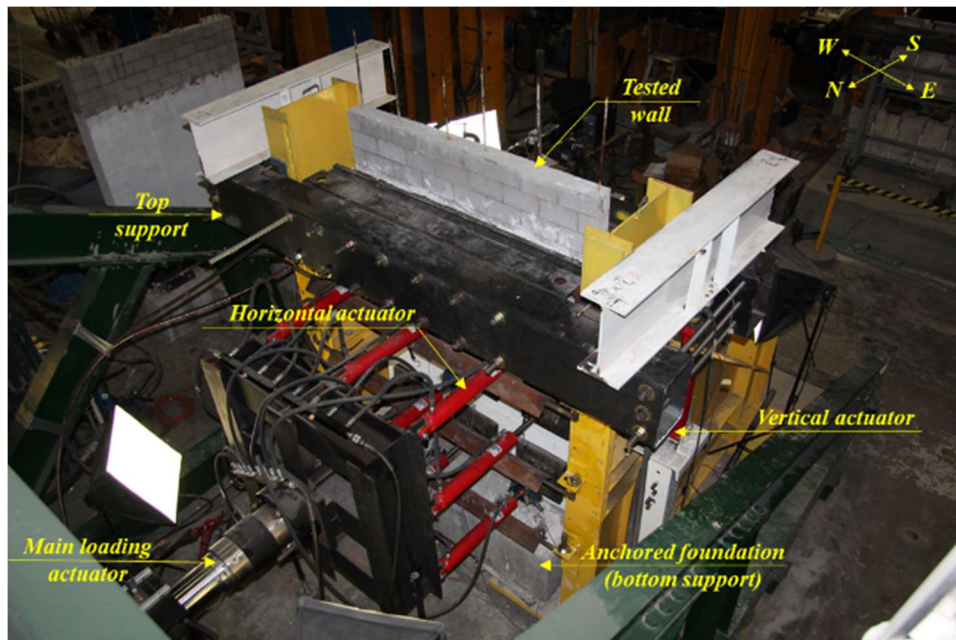

(a)

(b)

(c)

(d)

Figure 2 : Construction stages: (a) Reinforcement arrangement; (b) Half wall construction; (c) Half wall grouting; (d) Full wall construction

(a)

(b)

Figure 3: Test Setup: (a) 3D view for the test setup; (b) Loading and support system

The load-bearing walls were vertically (i.e. axially) loaded by a separate loading mechanism, through fitted threaded bars, using two hydraulic actuators. These two actuators were attached to the top (horizontal) support; which only restrained the horizontal deformation and vertically slid on the testing frame. High-performance polymers were used to reduce the friction between the testing frame and the top horizontal support. On the other side, the concrete foundations were attached to the testing frame using eight prestressed rods forming the bottom support. Figure 3 (a and b) depict the horizontal and vertical loading systems and the walls' fixation mechanism.

The horizontal and vertical deformations of the tested walls were monitored using displacement potentiometers. More specifically, the horizontal deformations were monitored through seven potentiometers (A, B, C1, D, E, F and G) to capture the out-of-plane deflection profile, and one redundant potentiometer (C_2) at the control station to be used in case of the malfunction of the main potentiometer (C_1). Three strain gauges were also attached to the vertical reinforcement bars at the foundation, mid-height, and at the top support, levels to monitor possible reinforcement yielding. Moreover, the load was verified through three diagonally load cells to monitor any loading misalignment, the wall axial load was monitored using two load cells attached to the two vertical actuators, as shown in Fig. 3a. Further details about the instrumentation and test setup can be found in Salem et al. (2019) [27].

The walls were loaded in a cyclic manner in the out-of-plane direction. the walls were loaded to reach targeted chord rotations (θ) (i.e. defined as the ratio between the Mid-height displacement and half the wall height) ($\theta= 1/8°$), then were unloaded until they reached zero loads. No strain hardening cycles were utilized in order to yield the monotonic response of the tested walls [28].

EXPERIMENTAL RESULTS AND OBSERVATIONS

Damage Sequence and Failure Modes
This subsection presents the damage sequence and the failure modes of the tested walls. All the walls showed similar crack patterns especially at their early loading stages, characterized by horizontal cracks at the first bed joint above the foundation at the front wall face followed by similar cracks at the mid-height of the rear wall face. This crack pattern is mainly attributed to the fixed support condition at the foundation level that localized more flexural stresses relative to those at the wall mid-height. This pattern is verified through the consistent strain propagation of the vertical bars, where the bar strain at the foundation level was not only always higher than that at the mid-height, but also exceeded the yield strain at an earlier stage of loading. At higher displacement levels, for all walls, the crushing started at the foundation level (rear face) before the wall reached its ultimate load. Subsequently, the wall experienced additional crushing at the mid-height of the front face, which was accompanied by a decrease in the wall load-carrying capacity. Fig. 4 depicts the cracking pattern in both the rear and the front faces of the tested walls
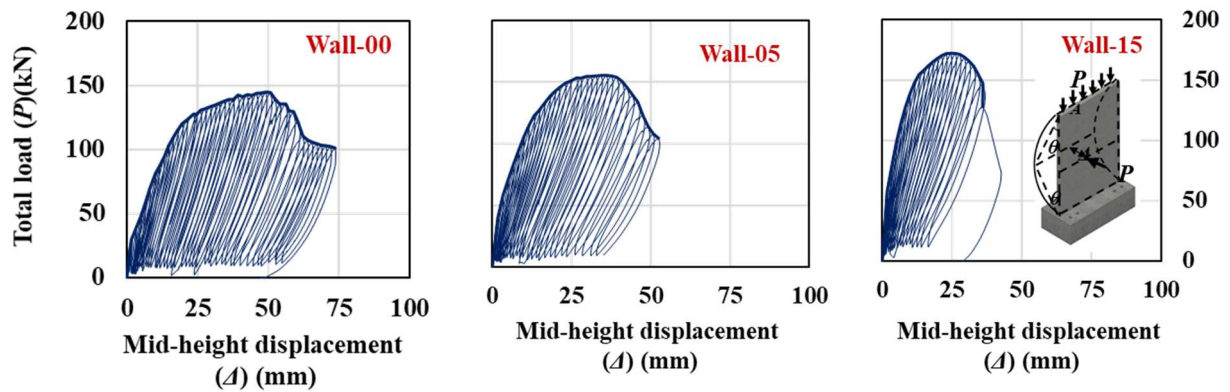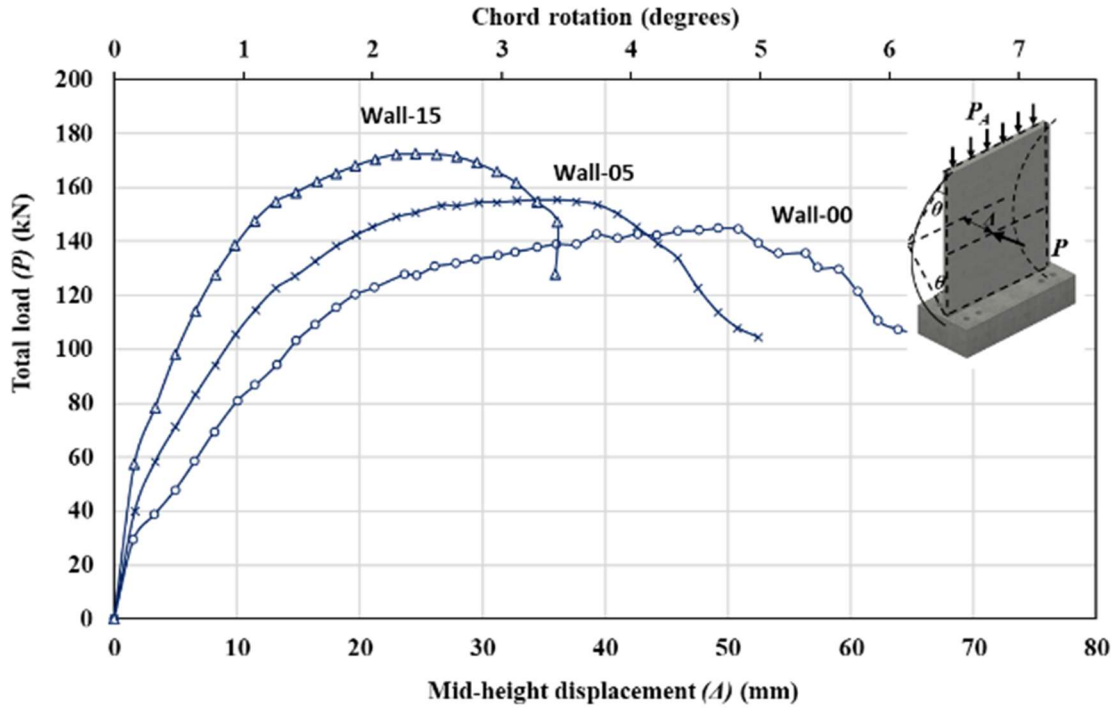
<div align="center">(a)   (b)</div>

Figure 4: Typical cracking pattern: (a) rear face; (b) front face

Load-displacement Behavior

Figure 4 shows the out-of-plane hysteretic load-displacement relationships for all the tested walls. In this figure, the total load, P, represents the resultant of the distributed loads acting on the wall loaded area (i.e. distributed through the nine secondary actuators), while the displacement, Δ, is measured at the mid-height of the wall (i.e. 750 mm from the foundation). While Figure 6 shows the resistance functions of the tested walls by illustrating their peak loads at each cycle with respect to the corresponding mid-height displacements and chord rotations. As can be observed from Fig. 6, all the tested walls did not show similar initial stiffness values due to their different axial stress levels. This is mainly attributed to the direct relation between the wall effective moment of inertia and the applied axial stress level [29].

Figure 5: Hysteretic behaviour for the tested walls

Figure 6: Load-deformation curves for the tested beams

ANALYSIS OF THE EXPERIMENTAL RESULTS

Secant Stiffness Degradation

Wall stiffness is key to model the inelastic wall behavior. In this respect, Fig. 7 presents the influence of the design parameters on the normalized secant stiffness (i.e. defined as the ratio between the wall secant stiffness (K_s) to its initial stiffness (K_i)) throughout the test. The figure shows a similar trend of stiffness degradation at low displacement levels, where the normalized secant stiffness values of all walls were reduced approximately by 30% at Δ=5mm. At higher displacement levels, the wall's axial load influences its normalized secant stiffness values. For example, the normalized secant stiffness of Wall-00 is 60% higher than that of Wall-15, respectively, at Δ= 35mm, as shown in Fig. 7.

Energy Dissipation

Energy dissipation (E_d) was determined by calculating the area enclosed by the resistance functions at different displacement levels, as shown in Fig. 8 [30]. The figure shows that E_d values were highly influenced by the axial stress. For example, Figure 8 shows that the E_d of Wall-15 increased by 43% at 36 mm, mid-height deflection, compared to Wall M-00. This is attributed to the direct dependency between these axial loads and the wall's flexural capacity. Although Wall-00 showed significant energy dissipation (at the ultimate stage) compared to Wall-15, the in-plane energy dissipation for both walls is expected to be significantly higher as observed by other researchers [31,32].
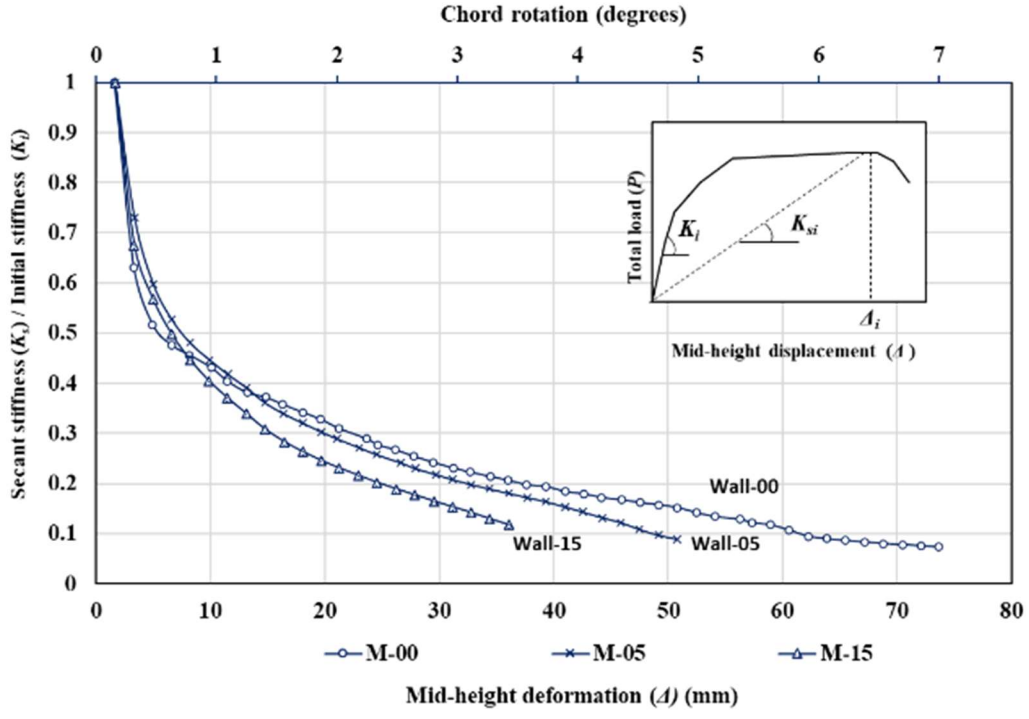
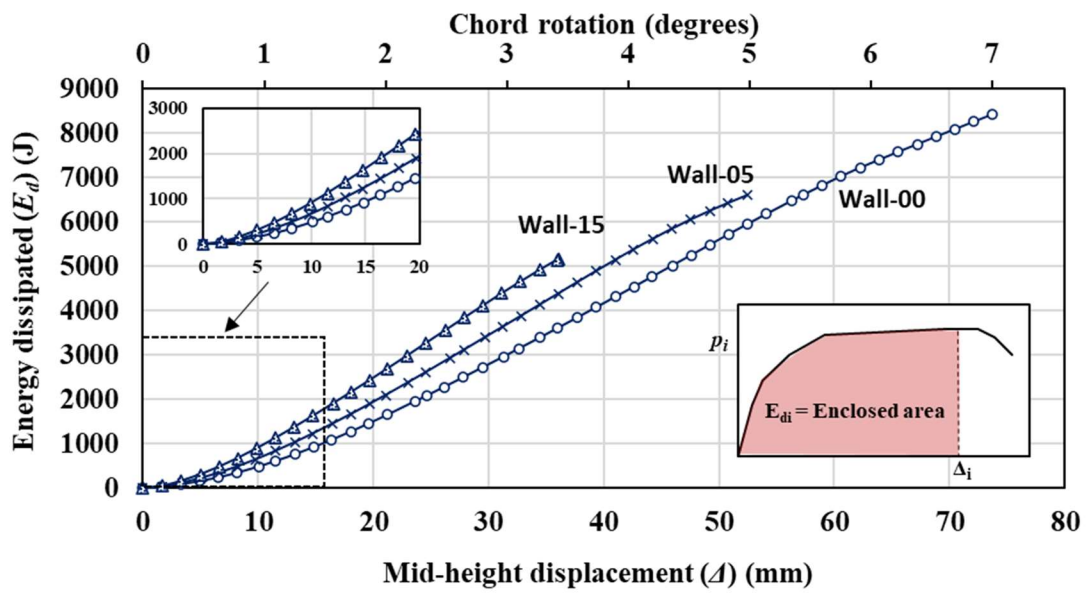**Figure 7: Secant stiffness degradation**

Figure 8: Energy dissipation propagation

CONCLUSIONS

The current study experimentally investigated the out-of-plane behavior of three half-scale fully grouted RMSWs subjected to a quasi-static unidirectional cyclic loading. The experimental results demonstrated that the axial stress influenced the out-of-plane performance of RM walls in terms of initial and secant stiffnesses, energy dissipation. The axial load increased the wall energy dissipation but reduced its corresponding normalized secant stiffness.

Although the current study presented an experimental investigation that covered different seismically detailed RMSWs, additional experimental tests are still required. These additional tests should cover different reinforcement ratios, boundary conditions, and axial load levels.

REFERENCES
[1] Priestley MJNMN, Calvi GM, Kowalsky MJ, Park T. Displacement-based seismic design of structures. Pavia, Italy: IUSS Press; 2007.
[2] CSA. CSA S304-14 Design of Masonry Structures. Mississauga, ON, Canada: Canadian Standards Association; 2014.
[3] The Masonry Society (TMS). Building Code Requirements for Masonry Structures. Detroit, MI: TMS 402-16/ACI 530-16/ASCE 5-16; 2016.
[4] ElSayed M, El-Dakhakhni W, Tait M. Response Evaluation of Reinforced Concrete Block Structural Walls Subjected to Blast Loading. J Struct Eng 2015;141:04015043. https://doi.org/10.1061/(ASCE)ST.1943-541X.0001239.
[5] Salem S, El-Dakhakhni W, Tait M. Robustness-Based Design of Reinforced Masonry Wall Buildings Under Blast Loading. Brick Block Mason 2016:1007–14. https://doi.org/10.1201/b21889-137.
[6] Bui TT, Limam A. Out-of-plane behaviour of hollow concrete block masonry walls unstrengthened and strengthened with CFRP composite. Compos Part B Eng 2014;67:527–42. https://doi.org/10.1016/j.compositesb.2014.08.006.
[7] Marjanishvili SM. Progressive Analysis Procedure for Progressive Collapse. J Perform Constr Facil 2004;18:79–85. https://doi.org/10.1061/(ASCE)0887-3828(2004)18:2(79).
[8] Bechara EA, Ahmad AH, Harrv GH. Flexural Behavior of Reinforced Concrete Masonry Walls under Out-of-Plane Monotonic Loads. ACI Struct J 1996;93. https://doi.org/10.14359/9692.
[9] Zhang X (David), Singh S, Bull DK, Cooke N. Out-of-Plane Performance of Reinforced Masonry Walls with Openings. J Struct Eng 2001;127:51–7. https://doi.org/10.1061/(ASCE)0733-9445(2001)127:1(51).
[10] Browning RS, Hoemann JM, Davidson JS. Large-Deflection Response of Fully Grouted Reinforced Masonry Walls to Static and Dynamic Out-of-Plane Pressure. ACI Spec Publ

2011;281:1–20. https://doi.org/10.14359/51683619.

[11] Browning RS, Davidson JS. Use of Empirical Constitutive Properties to Develop a Resistance Function for Reinforced Masonry. Struct. Congr. 2011, Reston, VA: American Society of Civil Engineers; 2011, p. 1310–9. https://doi.org/10.1061/41171(401)116.

[12] ElSayed M, El-Dakhakhni W, Tait M. Resilience Evaluation of Seismically Detailed Reinforced Concrete-Block Shear Walls for Blast-Risk Assessment. J Perform Constr Facil 2016;30:04015087. https://doi.org/10.1061/(ASCE)CF.1943-5509.0000742.

[13] Porto F, Mosele F, Modena C. Experimental testing of tall reinforced masonry walls under out-of-plane actions. Constr Build Mater 2010;24:2559–71. https://doi.org/10.1016/j.conbuildmat.2010.05.020.

[14] da Porto F, Mosele F, Modena C. Cyclic out-of-plane behaviour of tall reinforced masonry walls under P-Δ effects. Eng Struct 2011;33:287–97. https://doi.org/10.1016/j.engstruct.2010.10.004.

[15] Chang G, Mander J. Seismic Energy Based Fatigue Damage Analysis of Bridge Columns: Part I - Evaluation of Seismic Capacity. Tech Rep 94-0006 1994.

[16] Long L, Hamid A, Drysdale R. Small-scale modelling of concrete masonry using ½ scale units: a preliminary study. 10th Can 2005.

[17] ASTM. Standard Specification for Grout for Masonry. West Conshohocken, PA: ASTM C476-16; 2016.

[18] Heerema P, Shedid M, Konstantinidis D, El-Dakhakhni W. System-Level Seismic Performance Assessment of an Asymmetrical Reinforced Concrete Block Shear Wall Building. J Struct Eng 2015;141:04015047. https://doi.org/10.1061/(ASCE)ST.1943-541X.0001298.

[19] ACI committee 318. Building Code Requirements for Structural Concrete and Commentary (ACI 318M-14). Farmington Hills, MI: 2014.

[20] ASTM. Standard Test Methods for Sampling and Testing Concrete Masonry Units and Related Unit. West Conshohocken, PA: ASTM:C140/C140M-16; 2016.

[21] CSA. CSA A165-14, Standards on concrete masonry units. Mississauga, ON, Canada: Canadian Standards Association; 2014.

[22] ASTM. Standard Test Method for Preconstruction and Construction Evaluation of Mortars for Plain and Reinforced Unit Masonry. West Conshohocken, PA: ASTM C780 - 16a; 2016.

[23] CSA. CAN/CSA-A179-14, Mortar and Grout for Unit Masonry. Mississauga, ON, Canada: Canadian Standards Association; 2015.

[24] ASTM. Standard Test Method for Sampling and Testing Grout. West Conshohocken, PA: ASTM C1019-16; 2016.

[25] ASTM. Standard Test Method for Compressive Strength of Masonry Prisms. West Conshohocken, PA: ASTM C1314-16; 2016.

[26] CSA. CSA G30.18-09, Carbon steel bars for concrete reinforcement. Mississauga, ON, Canada: Canadian Standards Association; 2014.

[27] Salem S, Ezzeldin M, El-Dakhakhni W, Tait M. Out-of-Plane Behavior of Load-Bearing Reinforced Masonry Shear Walls. J Struct Eng 2019;145:04019127. https://doi.org/10.1061/(ASCE)ST.1943-541X.0002403.

[28] Applied Technology Council. Improvement of Nonlinear Static Seismic Analysis Procedures. Washington, D.C.: 2009.

[29] Paulay T, Priestley M. Seismic design of reinforced concrete and masonry buildings. New York: Wiley; 1992.

[30] Hose YD, Seible F. Performance Evaluation Database for Concrete Bridge Components and Systems under Simulated Seismic Loads. PEER Rep. No. 1999/11; 1999.

[31] Siyam MA, El-Dakhakhni WW, Banting BR, Drysdale RG. Seismic Response Evaluation of Ductile Reinforced Concrete Block Structural Walls. II: Displacement and Performance–Based Design Parameters. J Perform Constr Facil 2016;30:04015067. https://doi.org/10.1061/(ASCE)CF.1943-5509.0000804.

[32] Siyam MA, El-Dakhakhni WW, Shedid MT, Drysdale RG. Seismic Response Evaluation of Ductile Reinforced Concrete Block Structural Walls. I: Experimental Results and Force-Based Design Parameters. J Perform Constr Facil 2016;30:04015066. https://doi.org/10.1061/(ASCE)CF.1943-5509.0000794.